Am J Cancer Res 2024;14(5):2072-2087
www.ajcr.us /ISSN:2156-6976/ajcr0155379

Original Article

The small-molecule drug homoharringtonine targets HSF1 to suppress pancreatic cancer progression

Gui-Hong Li[1,2*], Ying Miao[3*], Huang Chen[3], Meng-Fei Xue[2], Jia-Yu Wang[3], Jing-Wen Zhang[3], Zheng-Fang Yi[3], Zhen-Liang Sun[2]

[1]School of Pharmaceutical Sciences, Southern Medical University, Guangzhou 510515, Guangdong, P. R. China; [2]Affiliated Fengxian Hospital, Southern Medical University, Shanghai 201499, P. R. China; [3]Shanghai Key Laboratory of Regulatory Biology, Institute of Biomedical Sciences and School of Life Sciences, East China Normal University, Shanghai 200241, P. R. China. [*]Equal contributors.

Received January 10, 2024; Accepted April 21, 2024; Epub May 15, 2024; Published May 30, 2024

Abstract: Heat shock factor 1 (HSF1), an essential transcription factor for stress response, is exploited by various tumors to facilitate their initiation, progression, invasion, and migration. Amplification of HSF1 is widely regarded as an indicator in predicting cancer severity, the likelihood of treatment failure and reduced patient survival. Notably, HSF1 is markedly amplified in 40% of pancreatic cancer (PC), which typically have limited treatment options. HSF1 has been proven to be a promising therapeutic target for multiple cancers. However, a direct small molecule HSF1 inhibitor with sufficient bioactivity and reliable safety has not been developed clinically. In this study, we successfully established a high-throughput screening system utilizing luciferase reporter assay specifically designed for HSF1, which leads to the discovery of a potent small molecule inhibitor targeting HSF1. Homoharringtonine (HHT) selectively inhibited PC cell viability with high HSF1 expression and induced a markedly stronger tumor regression effect in the subcutaneous xenograft model than the comparator drug KRIBB11, known for its direct action on HSF1. Moreover, HHT shows promise in countering the resistance encountered with HSP90 inhibitors, which have been observed to increase heat shock response intensity in clinical trials. Mechanistically, HHT directly bound to HSF1, suppressing its expression and thereby inhibiting transcription of HSF1 target genes. In conclusion, our work presents a preclinical discovery and validation for HHT as a HSF1 inhibitor for PC treatment.

Keywords: HSF1, pancreatic cancer, HHT, small molecule inhibitor, HSP90 inhibitor resistance

Introduction

Cancer cells are chronically subjected to a multitude of stressors, including metabolic reprogramming, proteotoxic stress, and genome damage [1, 2]. The maintenance and progression of the malignant phenotype necessitates the stabilization of oncogenic signaling proteins often characterized by conformational instability, including receptors, protein kinases and transcription factors [3]. Heat shock response (HSR) is a critical protective mechanism that allows cancer cells to thrive under adverse conditions [4].

Heat shock factor 1 (HSF1), a member of the heat shock factor (HSF) family, is a cytoplasmic transcription factor mastering HSR [5]. While in a dormant state as a monomer bound to chaperone proteins in normal cells, HSF1 becomes activated, oligomerizes, and translocates to the nucleus via diverse mechanisms when cells encounter stress [6, 7]. The transcriptional function of HSF1 relies on its DNA binding domain (DBD), which directly interacts with heat shock element (HSE) to control the expression of downstream genes [8]. HSF1 regulates a variety of downstream proteins, including protein-folding chaperones, cell cycle factors, DNA damage and repair proteins, as well as tumor microenvironment regulators [9]. Unlike other members of the HSF family, HSF1 is especially activated in many human cancers, positioning it as an indispensable intermediary transmitter within multiple oncogenic signaling pathways to drive unique oncogenic transcription programs for maintaining tumor survival [10-15]. Cancers are found to adapt “non-oncogene addiction” to

https://doi.org/10.62347/XFJH3424

HSF1 [16], and the expression of HSF1 is correlated with the outcomes of chemotherapy remission, disease-free survival, and the cancer severity in patients.

Pancreatic cancer (PC) is characterized by rapid metastasis and high lethality, primarily due to the severe shortage of early biomarkers and viable treatments. HSF1 is consistently expressed in intraductal papillary mucinous neoplasm (IPMN) and pancreatic intraepithelial neoplasias (PanINs) of PC, which facilitates the tumor progression to invasive and aggressive stages [17]. Approximately 40% of PC cases exhibit abnormal HSF1 expression [18]. HSF1 gene deletion increases the proportion of apoptotic cells, attenuates the proliferation, invasion, and migration of PC cells [19]. Moreover, HSF1 inhibition reverses gemcitabine chemotherapy resistance and suppresses tumor growth in gemcitabine-resistant animal models [13]. Therefore, HSF1 emerges as a promising therapeutic target for PC.

The development of inhibitors targeting HSF1 has presented considerable challenges. First, HSF1 exhibits limited 'druggability' traits due to the lack of potential target sites in its tertiary structure and its role as a ligand-free transcription factor [20, 21]. Second, HSF1 activation is complicated, involving multiple factors such as a multichaperone complex and numerous post translational modifications. Although considerable advances in creating novel HSF1 inhibitors have been achieved after decades of research, the progression of these agents is impeded by issues such as water solubility, toxicity, efficacy, and an incomplete understanding of their mechanisms.

In this study, we developed a high-throughput screening system for HSF1 inhibitors, through which homoharringtonine (HHT), a small-molecule inhibitor directly targeted HSF1, was successfully screened by luciferase reporter gene systems and MTS assays. Notably, HHT showed an affinity for binding with HSF1, leading to the suppression of HSF1 target genes expression, and a consequential reduction in the viability of PC cells with high HSF1 expression, which was achieved by inducing cell apoptosis and cycle arrest through DNA damage. Compared to KRIBB11, the first direct inhibitor of HSF1, HHT appeared better tolerated and considerably more effective in its anti-tumor activity *in vivo*. Our research highlights HHT as an HSF1 inhibitor with potential therapeutic values for PC.

Material and methods

Chemicals, cell lines and human tumor tissues

The small compounds, including HHT, KRIBB11, 17-AAG and NVP-AUY922, were purchased from MCE. Human PC cell lines, including CFPAC-1, MIAPACa-2, ASPC-1, BXPC-3, PANC-1 were generously provided by Shanghai Stem Cell Bank of Chinese Academy of Sciences and ATCC. Human embryonic kidney cell line (HEK293T) and human normal pancreatic ductal cell line (hTERT-HPNE) were sourced from the Meisen Cell Technology Co., LTD. Human PC tumor tissues were provided by Southern Medical University Affiliated Fengxian Hospital.

Cell line culture

PANC-1, CFPAC-1, MIAPACa-2, HPNE and HEK293T were cultured in Dulbecco's modified Eagle's Medium, while BXPC-3 and ASPC-1 were grown in RPMI 1640 medium. All media contained 1% penicillin streptomycin and 10%-15% fetal bovine serum (FBS). All cell lines were cultured at 37°C with 5% CO_2.

Screening strategy for HSF1 inhibitors

Every compound within the screening library must undergo a tiered evaluation process, beginning at the molecular level, followed by cellular level assessments. Firstly, a screening model based on luciferase reporter gene was constructed to the initial screening of all compounds of the screen library. Secondly, the IC_{50} of the compounds which enable to inhibit luciferase activity according to initial screening results to suppress PC cells proliferation were determined. The compound with the best molecular and cellular activity was selected as the target compound.

Luciferase reporter assay

10 μg pHSF1-Luc reporter plasmids (Yeasen Biotechnology) and 1 μg Renilla luciferase vectors were transiently co-transfected into HEK293T cells using PEI. Six hours after transfection, HEK293T was digested, collected, counted, and seeded in 96-well plates with 1×10^4 cells per well overnight. Then, the trans-

fected cells were pretreated with DMSO or HHT for 1 h, subjected to heat shock at 42°C for 25 min, and subsequently recovered at 37°C for 5 h. Finally, Dual-Luciferase Reporter Assay System (Promega) was used to evaluate the Renilla and firefly activities. Results were presented as the ratio of firefly to Renilla luciferase activity.

Western blot

Proteins from tissues and cells treated with drugs were extracted using RIPA buffer. Western blot was performed using primary antibodies against HSF1 (12972S, CST), HSP90 (4877S, CST), HSP27 (2402T, CST), BCL2 (T40056, Abmart), PARP (T40050, Abmart), BCL-XL (2764T, CST), CyclinD1 (ab134175, Abcam), CyclinB1 (CY5531, Abways), CDK4 (CY5836, Abways), p-CHK1 (2348T, CST), γH2AX (9718S, CST), p-STAT3 (T56566F, Abmart), c-Myc (55150F, Abmart), p-ERK (T40072F, Abmart), and GAPDH (ab0036, Abways). Secondary anti-rabbit 800 and mouse 800 (LI-C-OR Biosciences) antibodies provided visualization.

Cell viability

Briefly, PC cells were cultured into 96-well plates at appropriate confluence and allowed attachment overnight. Following a 72 h treatment with HHT, KRIBB11 or DTHIB exposure, 20 μL Aqueous One solution (MTS) was then added and further incubated at 37°C for 1-2 h. Cell OD values at 490 nm were measured using CellTiter-Glo (Promega, G3581) following the manufacturer's instructions and IC_{50} was calculated using GraphPad Prism 8.0.

Colony formation

PC cells were seeded into 6-well plates, allowed to adhere overnight, and then treated with a gradient of HHT, KRIBB11 or DTHIB concentrations for one week. The colonies were fixed by 4% paraformaldehyde for 30 min and then stained with 0.2% crystal violet for 1 h. Images were photographed using a digital camera, and colonies were counted manually.

Apoptosis assay

Apoptosis in PC cells treated with HHT for 48 h was quantified using the Apoptosis Detection Kit (Beyotime, C1062L). Then, cells were collected and resuspended in 1× binding buffers, followed by staining with Annexin-V fluorescein isothiocyanate and propidium iodide for 20 min in the dark room. Finally, samples were analyzed by flow cytometry (FACSCalibur, BD Biosciences).

Mitochondrial membrane potential staining assay

The JC-1 fluorescent staining kit (Beyotime, C2003S) was employed to evaluate alterations in mitochondrial membrane potential during apoptosis. Cells were seeded into 24-well plates at a density of 3×10^4 and cultured overnight at 37°C followed by treating with DMSO or 30 nM HHT for 48 h. After incubation, cells were washed twice with PBS and cultured with 0.5 ml of JC-1 working solution at 37°C for 20 min. Cell fluorescence images were collected using fluorescence microscopy (EClassical 3100, Echo, USA).

Cell cycle assay

Cell cycle was assessed by the Cell Cycle and Apoptosis Analysis Kit (Beyotime, C1052). Flow cytometry was used to determine the effect of HHT on cell cycle. Cells were seeded into 6-well plates and treated with varying concentrations of HHT for 48 h. Subsequently, the cells were centrifuged at 1000 rpm for 3 min, washed twice with PBS, and fixed in 70% ethanol that was pre-chilled to 4°C, and allowed to fix overnight. After that, cells were stained with PI staining solution and detected by flow cytometry (FACSCalibur, BD Biosciences).

Immunofluorescence staining

Immunofluorescence was conducted using DNA damage kit (Beyotime, C2035S). Post-treatment for 48 h, PC cells were rinsed with cold PBS, fixed with fixing solution for 15 min. After blocking at room temperature for 20 min, cells were further incubated with the primary antibody at 4°C overnight. The following day, cells were incubated with secondary antibody at room temperature for 1 h and then DAPI staining was performed. Fluorescence images were captured with an EClassical 3100 microscope (Echo, USA).

Transient transfection small interfering RNA (siRNA)

PC cells were seeded into 6-well plates and transfected with HSF1 siRNA along with corre-

sponding controls (siNC) using Lipofectamine 3000. Following a 48 h transfection period, western blot was performed to verify the efficiency of HSF1 knockdown. Subsequently, apoptosis rate and mitochondrial membrane potential were performed to compare differences between siNC and siHSF1 group. The gene-specific siRNA is listed as follows:

Target Name	Target sequence
siHSF1	S: 5'CACAUUCCAUGCCCAAGUATT3'
	AS: 5'UACUUGGGCAUGGAAUGUGTT3'

HSF1 stable knockdown

The HSF1 gene-silenced plasmids were purchased from Shanghai GenePharm CO., Ltd. HSF1 shRNA was co-transfected with package plasmids pMD2G and pXPAX2 into HEK293T cells using PEI. After 72 h of transfection, the lentiviruses were collected and infected PANC-1 and MIAPACa-2. Then, 2 mg/ml puromycin was added to select stable HSF1 knockdown cells. Finally, the knockdown efficiency was measured by western blot.

Cellular thermal shift assay (CETSA)

MIAPACa-2 cells, treated with 10 μM HHT or DMSO for 1 h, were collected using PBS supplemented with the same initial treatment concentration. Then, the cell resuspension was aliquoted into different 0.2 ml EP tubes, heat on a PCR apparatus (Eppendorf) for 3 min according to the preset gradient heating program, and freeze-thaw repeatedly at liquid nitrogen and 37°C for 3 times. Finally, the samples were centrifuged, and the supernatant was analyzed by western blot.

Microscale thermophoresis assay

The binding affinity of HHT to purified full length HSF1 was measured using a Monolith NT.115 (NanoTemper Technologies). The RED fluorescent dye was used to label HSF1 protein following the manufacturer's procedure, and HHT was prepared at 16 serial dilutions using a two-fold gradient. Equal volumes of the labeled protein and each HHT concentration were combined. The samples were loaded into premium capillaries (NanoTemper Technologies) and measured at 25°C using 40% light-emitting diode and medium MST power. Data analyses were carried out using MO. Afnity Analysis v.2.2.4 software.

RNA sequencing

MIAPACa-2 cells were treated with either DMSO or 30 nM HHT for 36 h. Subsequently, RNA was extracted and collected for transcriptome gene sequencing, which was performed by Shanghai Majorbio Bio-pharm Technology Co., LTD.

Pancreatic tumor xenograft model

The MIAPACa-2 xenograft tumor models were established by subcutaneously injecting 1 × 10^7 MIAPACa-2 cells, suspended in PBS containing 50% Matrigel, into the right flank of a BALB/c-nude mouse. When the tumor volume reached 100-200 mm^3, all tumor-bearing mice were randomly divided into four groups for intraperitoneal treatment with DMSO (control group), 50 mg/kg KRIBB11 (KRIBB11 group), 1 mg/kg HHT (HHT-1 group) and 2 mg/kg HHT (HHT-2 group) respectively. Tumor volume and mouse body weight were recorded every four days, calculating tumor volume with the formula: tumor volume (V) = length × width × width × 0.52. Upon concluding the experiment, the mice were euthanized using CO_2. Tumors were harvested for western blot and immunohistochemistry analysis.

Immunohistochemistry

Briefly, tumor samples from xenograft models were fixed overnight with 4% PFA at 4°C. The sections were incubated with primary antibodies against HSF1, HSP27, γH2AX and Ki-67 at 4°C. In the second day, sections were detected with anti-rabbit or anti-mouse secondary antibodies. The signal was amplified and visualized using avidin-biotin complex (ABC) system and DAB substrate. Images were captured using a Leica photomicroscope.

Hematoxylin and eosin stain

The mouse organs were embedded in paraffin and sectioned into 4 μm slices. After dehydration through an ethanol gradient, sections were stained with hematoxylin, differentiated in 1% hydrochloric acid alcohol, and then stained with eosin for 5 seconds. Slides were sealed with neutral resin and imaged.

Statistical analysis

Experiments were repeated at least three times. Data analysis was performed by stu-

dent's T-test. Considering *p*-values < 0.05 as statistically significant. Differences between the control and experimental groups were evaluated by one-way ANOVA. Results are reported as mean values with 95% confidence intervals, and significance was set at P < 0.05. All data were analyzed using Microsoft Excel 2019 and GraphPad Prism 8.0.

Results

Identification of HHT as a small molecule HSF1 inhibitor

Previous reports have implicated HSF1 in regulating important processes, including chemotherapy resistance, microenvironment remodeling, and the formation of precancerous lesions [17, 22, 23]. The role of HSF1 in various cancers were further elucidated by analyzing the RNA-seq expression of HSF1 in CCLE database. As shown in **Figure 1A**, HSF1 was found to be abnormally high in a range of tumor cell lines, with the highest expression in PC cell lines. HSF1 plays a crucial role in accelerating epithelial mesenchymal transformation and PanIN formation [17, 24], with PanINs frequently progressing to pancreatic ductal adenocarcinoma (PDAC). Therefore, HSF1 is considered to be an indispensable driver in the progression of PC. We performed immunohistochemistry and confirmed substantial HSF1 accumulation in clinical PDAC patient samples from Southern Medical University Affiliated Fengxian Hospital (**Figure 1B**). Comparative analysis using the TCGA database revealed that PDAC tumors (n=179) express higher levels of HSF1 than adjacent normal tissues (n=171) (**Figure 1C**). Subsequently, the prognostic role of HSF1 in the survival of PDAC patients was evaluated. PDAC patients were divided into high HSF1 expression group (n=45) and low HSF1 expression group (n=45) according to the data obtained from TCGA database. Then the disease-free survival rate of patients in each group was analyzed. As shown in **Figure 1D**, patients with high HSF1 expression had a lower disease-free survival rate, indicating that HSF1 expression was significantly correlated with poor prognosis. In summary, aberrant HSF1 activation is intimately linked with disease progression and poor prognosis of PC patients, highlighting the clinical imperative for direct HSF1 targeting.

To identify an HSF1 inhibitor, we developed a screening strategy using dual luciferase reporter gene system and MTS assay as depicted in **Figure 1E**. A heat shock dependent luciferase reporter plasmid pHSF1-Luc and an internal control Renilla plasmid were co-transfected into HEK293T cells, and the cells were exposed to 44°C to stimulate the expression of endogenous HSF1. The validity and efficacy of this model were confirmed using KRIBB11, a known direct HSF1 inhibitor, as a benchmark, as a positive drug. Upon heat shock exposure, there was an approximate 20-fold rise in luciferase activity, and KRIBB11 displayed a dose-dependent suppression in response to the intensity of this model's stimulation (**Figure 1F**). By screening our internal small molecule compounds chemical library by using the successfully constructed model, we identified several potential candidate compounds (Figure S1A, S1B). HHT emerged as a promising candidate, as significantly inhibiting luciferase activity at very low concentrations (**Figure 1G**, **1H**).

Loss of HSF1 induces pancreatic cancer cell proliferation inhibition, apoptosis and mitochondrial membrane potential changes

In order to explore whether HSF1 amplification contributes to the proliferation of PC cells, PANC-1 and MIAPACa-2 were selected to knockdown the endogenous HSF1 by shHSF1, resulting in the creation of two stable HSF1-depleted cell lines (**Figure 2A**). Knockdown of HSF1 markedly inhibited cells colony formation (**Figure 2B**, **2C**). Moreover, HSF1 depletion significantly impaired the proliferative capacity of PC cells (**Figure 2D**, **2E**). To further verify the role of HSF1 on cell viability and apoptosis, HSF1 was transiently silenced in PC cells using siRNA (Figure S2A), which induced cell apoptosis of PANC-1 and MIAPACa-2 (**Figures 2F**, S2B). Since cell apoptosis partly originates from the loss of mitochondrial membrane potential [25], we utilized JC-1 fluorescent staining kit to assess whether changes existed in mitochondrial membrane potential in siHSF1 group. Indeed, compared to siNC group, the green fluorescence (JC-1 monomers) was increased and red fluorescence (JC-1 aggregates) was decreased in siHSF1 group (**Figure 2G**, **2H**). In summary, the proliferation of PC cells strongly depended on HSF1.

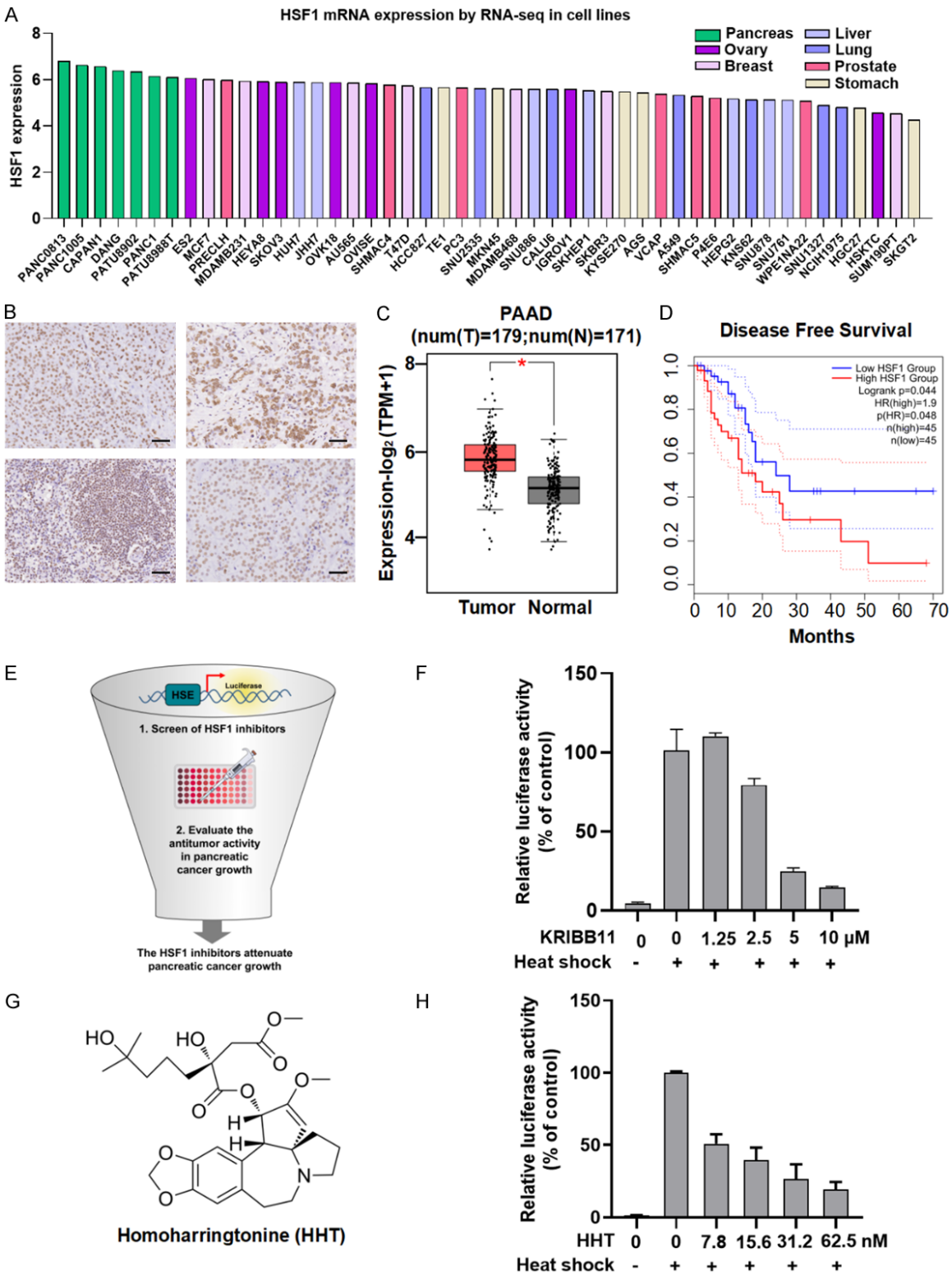

Figure 1. Identification of HHT as a small molecule inhibitor targeting HSF1. A. RNA-seq data showing relative HSF1 expression levels across various tumor cell lines, sourced from the CCLE database. B. The expression of HSF1 in clinical pancreatic ductal adenocarcinoma patients. Scale bar, 50 μm. C. Comparative analysis of HSF1 in two PC cohort pancreatic ductal adenocarcinoma (n=179) and paracancer tissues (n=171). D. Kaplan-Meier survival curves correlating patient survival with high (red) and low (blue) HSF1 expression levels, stratified by HSF1 expression with *p*-values from Log-rank test; n=45 per group. E. Screening strategy to identify small molecule HSF1

inhibitors for the PC treatment. F. Luciferase reporter plasmid and Renilla plasmid were transiently transfected into HEK293T. KRIBB11 was added for indicated concentration and luciferase activity was measured as materials and methods described. G. The chemical structure of HHT. H. Inhibitory activities of HHT on HSF1 luciferase reporter gene assay (n=3).

HHT targets HSF1 to inhibit pancreatic cancer cell proliferation

Differential expression of HSF1 was noted across various PC cell lines. Specifically, PANC-1, MIAPACa-3, CFPAC-1, and ASPC-1 cells demonstrate a significantly high expression of HSF1 while BXPC-3 and normal ductal cell HPNE display a low expression of HSF1 (**Figure 3A**). To evaluate the efficacy of HHT against PC, cells were incubated with HHT for 72 h. Cell viability results indicated that cell lines with high HSF1 expression were highly sensitive to HHT, while BXPC3 and HPNE were moderately sensitive to HHT (**Figure 3B**). Remarkably, HHT's activity was found to be more than 100 times that of the positive control drugs, KRIBB11 and DTHIB (Figure S3A-C). To examine whether HSF1 was the primary target of HHT, PANC-1 and MIAPACa-3 stably expressed HSF1 shRNA (shHSF1) or negative control shRNA (shNC) were exposed to HHT. Cells with HSF1 knockdown showed reduced sensitivity to HHT compared to their shNC counterparts (**Figure 3C**, **3D**). Furthermore, we carried out a fit-molecular docking experiment to predict the main binding modes of HHT and HSF1. HHT interacts with several crucial residues of HSF1-DBD, such as GLN73, TYR76, PHE61, ALA17, and LYS31 (**Figure 3E**). Last, drug-protein interaction experiment was performed to demonstrate whether HHT directly bound to HSF1. MIAPACa-3 was treated with HHT or DMSO for 1 h followed by cell lysates collection. In comparison to the DMSO control, HSF1 began to degrade at higher temperatures in the HHT-treated group (**Figure 3F**), suggesting that HHT can directly interact with HSF1, enhancing its thermal stability. In MTS assays, HHT directly bound HSF1 with K_D of 29.5 μM (**Figure 3G**). In conclusion, HHT directly targets HSF1 to inhibit the proliferation of PC cells.

HHT regulates downstream gene function via HSF1 and mitigates amplified HSR by HSP90 inhibition

Our previous work proved that cells with low HSF1 expression or HSF1 deletion was less sensitive to HHT. Then the inhibitory function of HHT on heat shock pathway was explored. First, we conducted RNA-seq analysis to compare the whole-transcriptome gene expression between control group and HHT treatment group. As shown in volcano map, HHT altered the transcriptional patterns of MIAPACa-2: 2424 genes were upregulated, and 2484 genes were downregulated after HHT treatment (**Figure 4A**). Notably, the expression of HSF1-regulated genes was substantially affected by HHT treatment (**Figure 4B**). Cells can counteract proteomic upheaval and defend against thermal stress, oxidative harm, and hypoxia by elevating their levels of HSPs through a compensatory stress response mechanism. Next, the level of heat shock proteins in PANC-1, MIAPACa-2 and ASPC-1 were analyzed by western blot 48 h post HHT treatment. HSF1 and its chaperone proteins HSP90 and HSP27 were reduced with the increasing HHT concentrations (**Figure 4C**).

Previous extensive research on HSP90 inhibitors, despite robust preclinical and clinical explorations backed by mechanistic insights, suggests limitations in their therapeutic use due to HSF1 activation following HSP90 inhibition [26, 27]. As our experiments confirmed, 17-AAG and NVP-AUY922 effectively inhibited the expression of HSP90 client proteins including p-STAT3, p-ERK and c-Myc, but activated HSF1 in PC cells (Figure S4A, S4B). This trend was reversed by HHT (**Figure 4D**, **4E**), positing HHT as a viable candidate to overcome resistance to HSP90 inhibitors.

HHT inhibits cancer cell viability by inducing apoptosis and mitochondrial membrane potential changes

Colony formation experiment was conducted to determine whether PC cell proliferation was affected by HHT. As expected, HHT significantly reduced cell colony formation ability of PANC-1, MIAPACa-2 and ASPC-1, with the most pronounced effects observed at high concentration (**Figures 5A**, S5A). Compared with the positive drug KRIBB11 and DTHIB, which showed bioactivity at micromole concentrations, HHT's inhibitory effect was over 100-fold greater (**Figures 5B**, S5A-C). To verify whether HHT

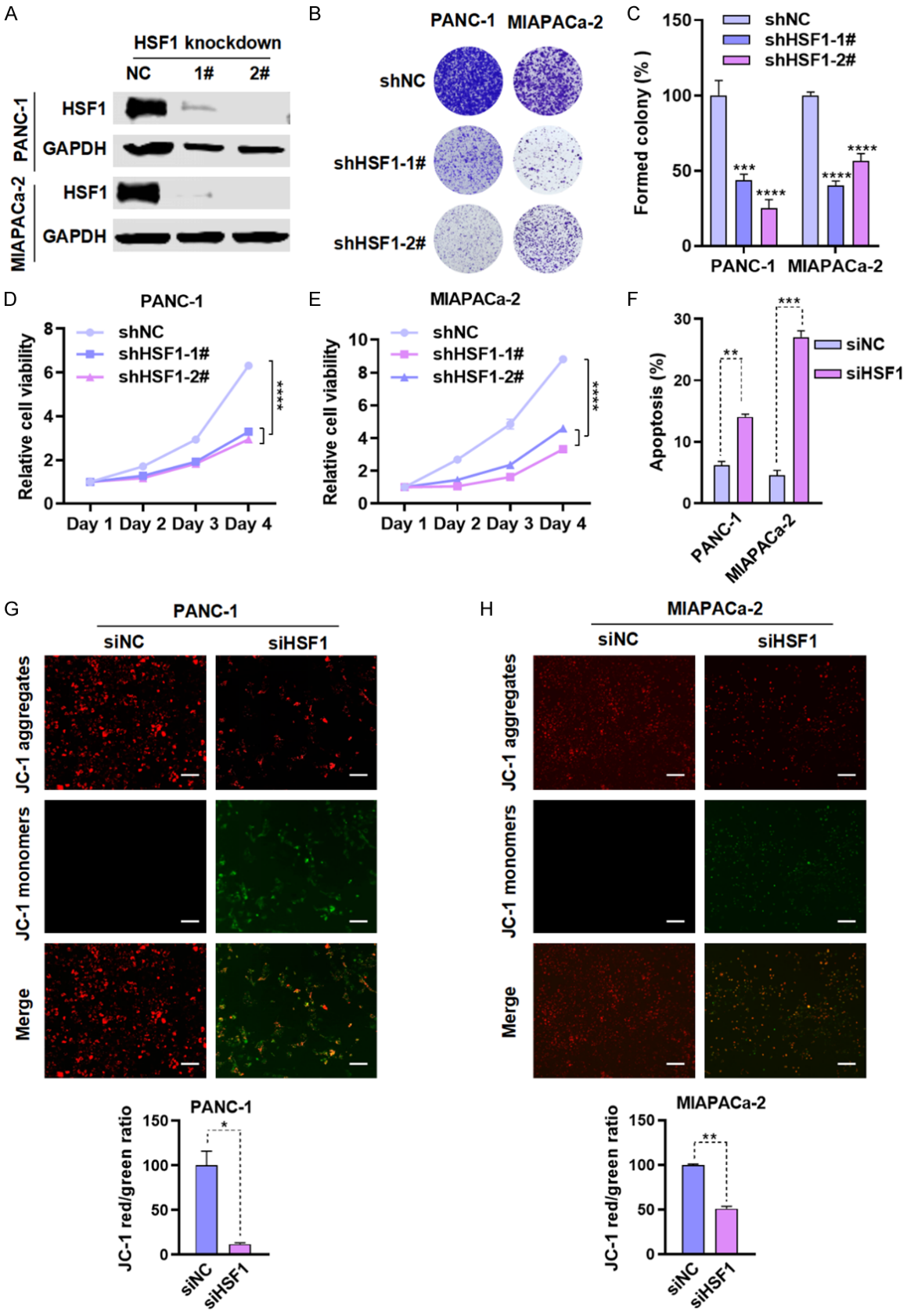

Figure 2. Loss of HSF1 induces pancreatic cancer cell proliferation inhibition, apoptosis and mitochondrial membrane potential changes. A. Verification of HSF1 knockdown efficacy in PC cells by western blot. B, C. PC cells stably

transfected with vector control or HSF1 small hairpin RNAs, the colony formation of different groups was detected. D, E. Growth inhibition in PC cells following HSF1 knockdown, with statistically significant variance between shNC and shHSF1 groups across two cell lines. Data are expressed as mean±SD, ****P < 0.0001 by one-way ANOVA followed by multiple comparisons. F. Loss of HSF1 induced cell apoptosis of PC cells. G, H. PANC1-1 and MIAPACa-2 cells were transfected with or without HSF1 siRNA and stained with JC-1. Scale bar, 100 μm.

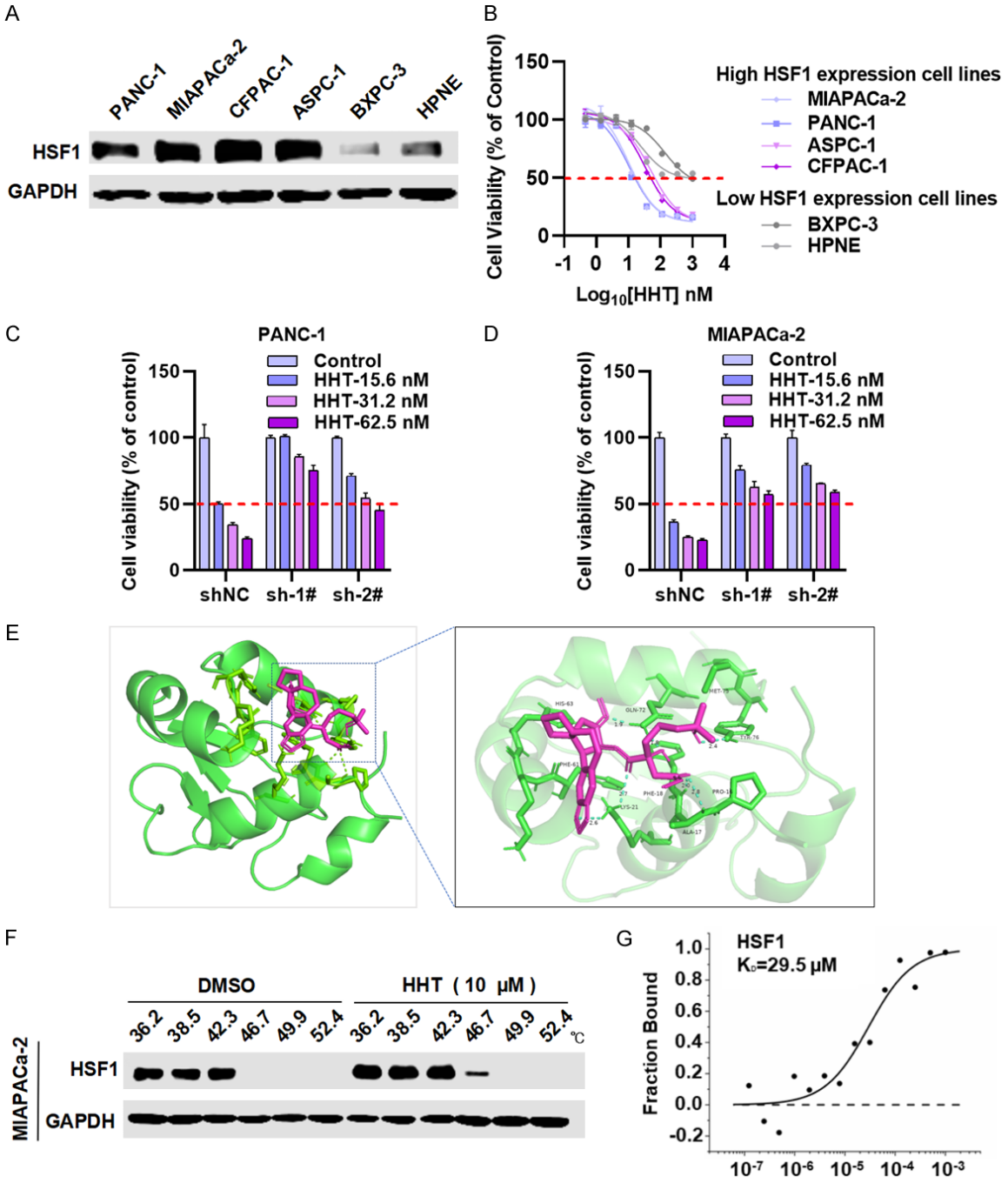

Figure 3. HHT targets HSF1 to inhibit pancreatic cancer cells proliferation. A. HSF1 expression assessed by western blot across 6 PC cell lines. B. HHT selectively inhibited PC cells growth with high HSF1 expression, as determined by MTS assay (n=3). C, D. HHT was less effective in the HSF1 knockdown PC cells. E. Schematic of molecular docking showing potential binding mode of HHT to HSF1 DBD. F. Cellular thermal shift assay (CETSA) of HSF1 with HHT treatment in MIAPACa-2. G. HHT bound to HSF1 and the binding affinity was quantitatively assessed by MTS experiments (n=3).

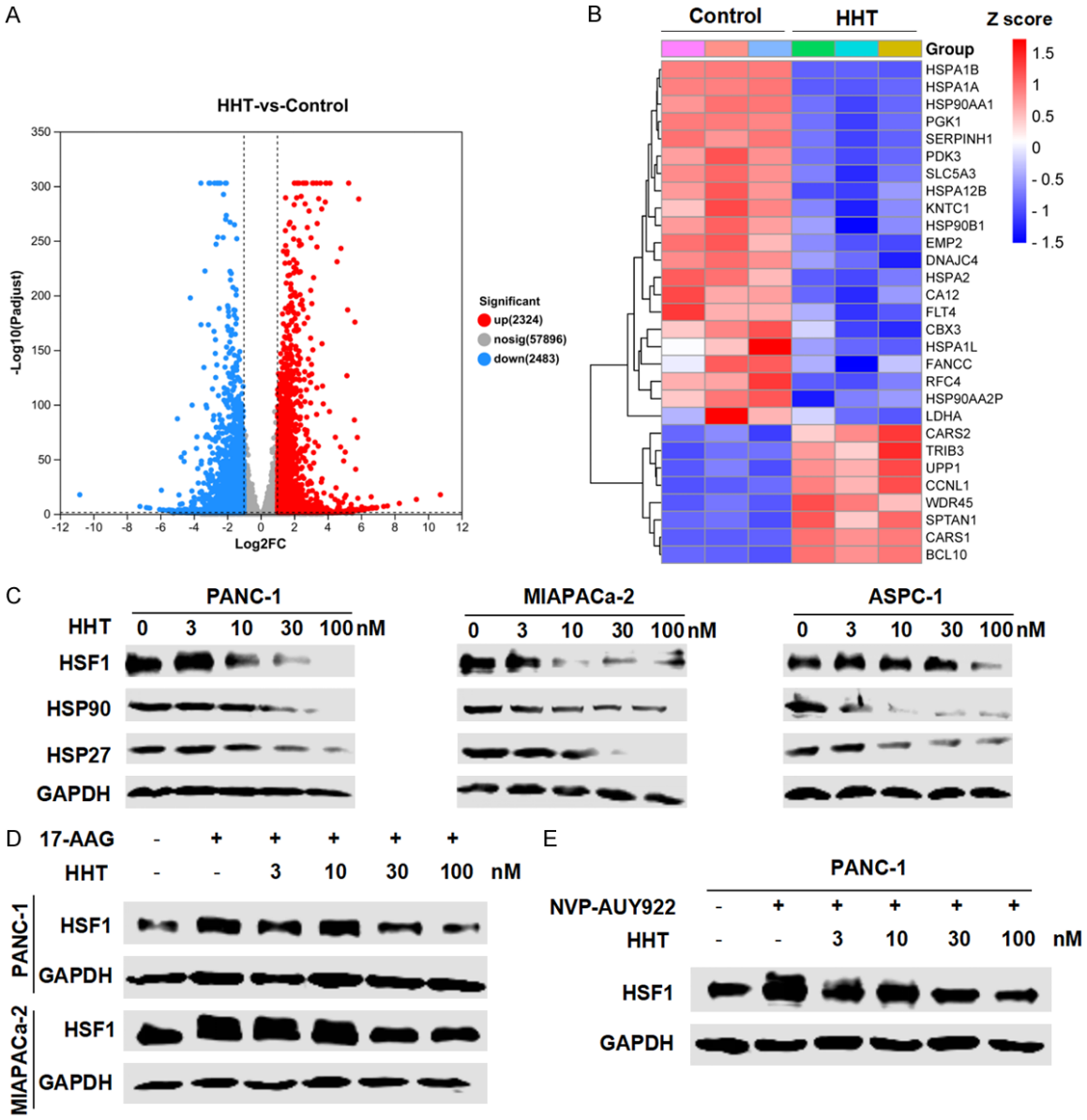

Figure 4. HHT regulates downstream gene function via HSF1 and mitigates amplified HSR by HSP90 inhibition. A. RNA-seq volcano map indicated genes altered by HHT. B. HSF1 target genes were significantly changed post HHT treatment. C. HHT treatment reduced the expression of HSF1, HSP90, and HSP27. D. HHT inhibited the expression of HSF1 which was induced by 17-AAG in PC cells. E. HHT inhibited the expression of HSF1 which was induced induced by NVP-AUY922 in PANC-1.

attenuated the proliferation of PC cells by increasing rates of apoptosis, FACS was used to analyze cell status. As shown in **Figures 5C**, **5D** and S5D, both PC cells showed an increased apoptosis rate caused by HHT. Western blot revealed a dose-dependent reduction in BCL2 and BCL-XL, and an increase in Cleaved-PARP, suggesting an upregulation of apoptosis (**Figure 5E**, **5F**). Consistently, compared to untreated group, the green fluorescence (JC-1 monomers) was increased and red fluorescence (JC-1 aggregates) was decreased in HHT group (**Figures 5G**, **5H**, S5E, S5F), similar to the effects of HSF1 deletion.

HHT treatment induces DNA damage, cycle checkpoint kinase activation, and cell cycle arrest

To explore the pattern of PC cell death triggered by HHT, we focused on its effect on cell cycle progression. Compared with untreated cells,

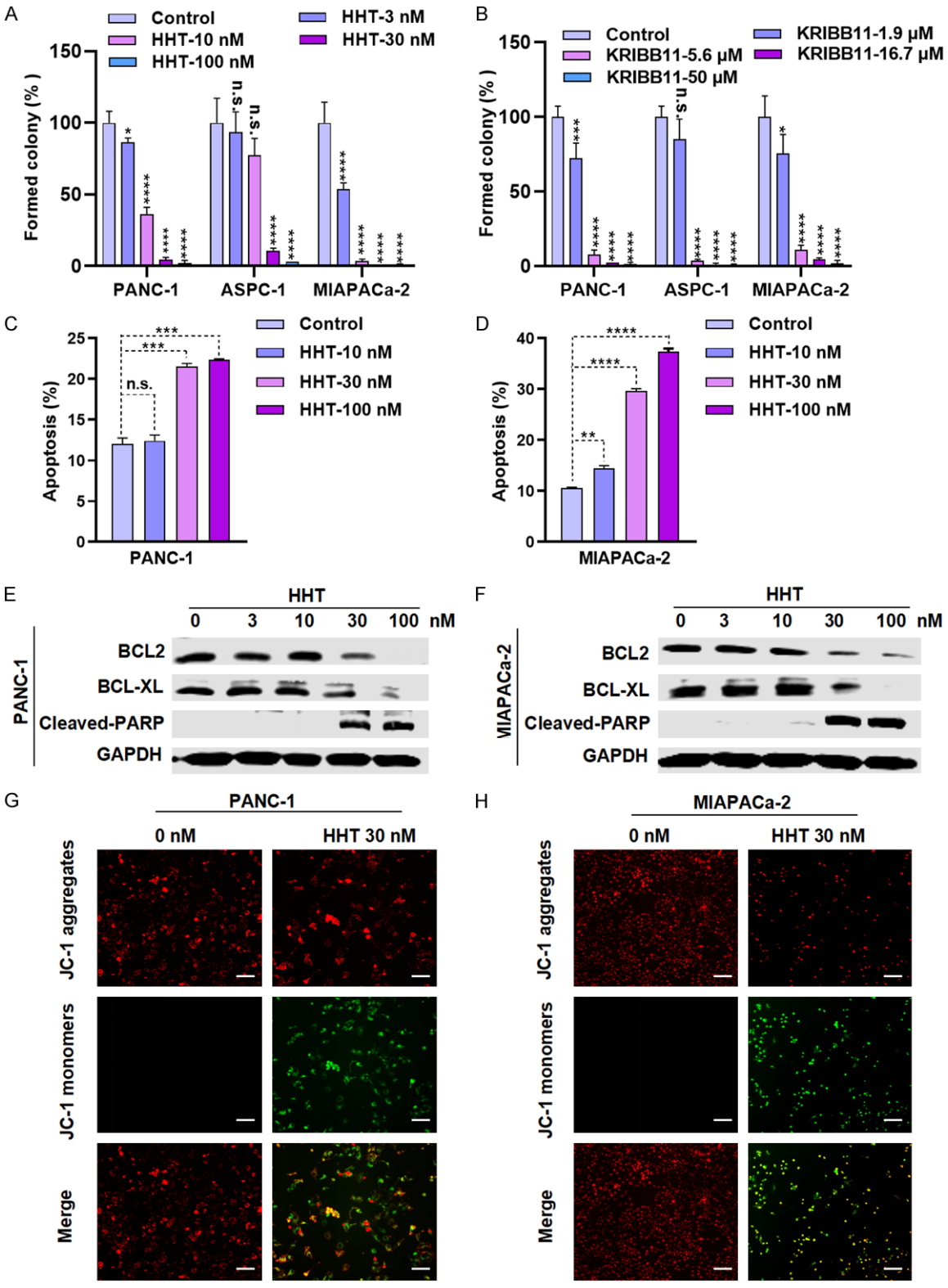

Figure 5. HHT inhibits cancer cell viability by inducing apoptosis and mitochondrial membrane potential changes. A, B. HHT and KRIBB11 inhibited PC cells colony formation. PC cells were seeded in 6-well plates and treated with indicated concentrations of HHT and KRIBB11. C, D. Apoptosis induction in PANC-1 and MIAPACa-2 cells by HHT, as detected by flow cytometry. E, F. Expression of apoptotic markers post-48-hour HHT treatment, as determined by western blot. G, H. PANC1-1 and MIAPACa-2 were treated with or without 30 nM HHT for 48 h and stained with JC-1. Scale bar, 100 μm.

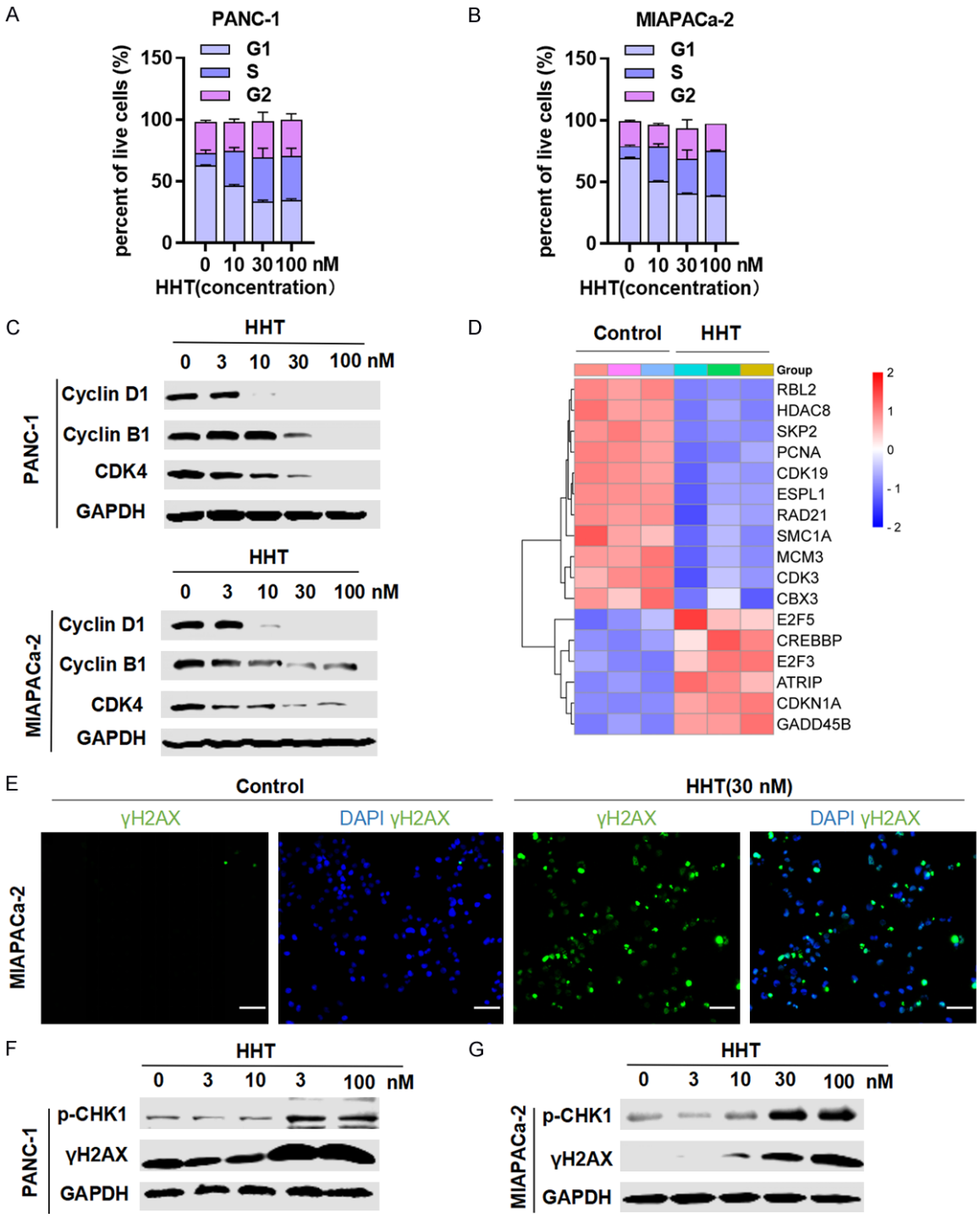

Figure 6. HHT treatment induces DNA damage, cycle checkpoint kinase activation, and cell cycle arrest. A, B. Statistical analysis of the impact of HHT on cell cycle distribution in PANC-1 and MIAPACa-2. C. Cell cycle factors were analyzed by western blot after HHT treatment. D. Heatmaps from RNA-seq indicating cell cycle genes regulated by HHT. E. Immunofluorescence staining of DNA damage marker γH2AX in MIAPACa-2. The γH2AX antibody (green) and DAPI (blue) were used for staining γH2AX and the nucleus, respectively. The stained samples were subsequently imaged and subjected to analysis. Scale bar, 50 μm. F, G. HHT caused DNA damage and CHK pathway activation in PC cells.

treatment of 100 nM HHT for 48 h resulted in a higher percentage of S phase: PANC-1 cells increased from 9.81% to 35.80%, and MIAPACa-2 from 9.57% to 36.85%. PANC-1 and

MIAPACa-2 were arrested in S phase by HHT in a dose-dependent manner (**Figures 6A**, **6B**, S6A). Key regulators of the cell cycle were affected, the expression levels of cell cycle proteins, including cyclin D1, cyclin B1, and CDK4, decreased with increasing concentrations of HHT (**Figure 6C**), disrupting the normal mitotic process. Further, as shown in heat maps generated from RNA-seq, HHT affected the RNA levels of numerous genes associated with the cell cycle (**Figure 6D**). Then, we explored the mechanism of cell cycle arrest induced by HHT. Immunofluorescence experiments revealed increased accumulation of γH2AX in MIAPACa-2 cells treated with HHT, indicating enhanced DNA damage (**Figures 6E**, S6B). In addition, p-CHK1 was increased after HHT treatment (**Figure 6F**, **6G**), suggesting the activation of cell DNA repair pathway which is responsible for cycle arrest during mitosis and allows cell to have enough time to repair damaged DNA. In brief, HHT caused DNA damage response and activated cell repair pathway to promote cell cycle arrest.

HHT blocks pancreatic cancer growth in vivo

On the basis of the potent inhibitory effects of HHT against HSF1-dependent PC cells, we proceeded to establish MIAPACa-2 subcutaneous tumor-bearing mode of BALB/c-nude mice to confirm the growth inhibition effect in *vivo* (**Figure 7A**). Treatment with 1 mg/kg/day and 2 mg/kg/day HHT markedly suppressed pancreatic tumor growth in the MIAPACa-2 xenograft model (**Figure 7B**). After 24 days drug administration, tumors were weighted, with HHT demonstrating a significantly greater inhibition of PC growth compared to KRIBB11 (**Figure 7C**, **7D**). Weight monitoring of the mice indicated that both HHT doses did not lead to substantial body weight loss (Figure S7A). Moreover, HHT was well-tolerated as lack of obvious toxicity in major organs, demonstrated by hematoxylin and eosin staining (Figure S7B, S7C). HHT inhibited the expression of HSF1 in *vivo* (**Figure 7E**), and indicators of genetic damage and cell apoptosis, such as Cleaved-PARP and γH2AX, were increased in HHT-treated tumor samples compared to the control group (**Figure 7E**). Immunohistochemical analyses reinforced the downregulation of HSF1 and HSP27 and the upregulation of γH2AX in the HHT-treated groups (**Figure 7F**). Ki-67, a proliferation marker, was markedly reduced by HHT in MIAPACa-2 xenograft model (**Figure 7F**). In summary, HHT was well-tolerated in mice and potently suppressed pancreatic tumor growth in *vivo*, outperforming the positive control agent, KRIBB11.

Discussion

Pancreatic cancer (PC) remains one of the most lethal malignancies, notoriously resistant to existing therapeutic modalities. Acknowledged as an incurable malignant tumor, the 5-year survival rate for advanced PC is only approximately 3.1% [28, 29]. Hence, there is an urgent need for developing new targets in the effective treatment of PC. HSF1 has emerged as a promising therapeutic target for PC due to its role in inducing tumor microvascularization, promoting tumor recurrence, and serving as a prognostic indicator for patient outcomes [30-32]. Additionally, studies have revealed a substantial elevation of HSF1 in PC cells resistant to gemcitabine [33]. Despite extensive research endeavors, direct targeting HSF1 with small molecules has been proven to be very challenging. KRIBB11, an inhibitor identified via luciferase reporter screening, inhibits HSF1-dependent p-TEFb recruitment, but exhibits limited efficacy in breast cancer, colon cancer and PC when used as a monotherapy. Another inhibitor, DTHIB, which binds to HSF1 DBD and accelerates degradation of nuclear HSF1 via the proteasome pathway, is effective only at high micromolar concentrations, hindering its clinical use. Therefore, the development of a potent, selective, and highly effective direct inhibitor for HSF1 remains underway. Here, we identify a potent HSF1 inhibitor, which exhibited more potency in suppressing PC growth in *vitro* and in *vivo*. HHT was found to trigger apoptosis and cell cycle arrest through DNA damage, diminish mitochondrial membrane potential, and initiate apoptosis. It also led to DNA damage, culminating in cell cycle arrest in the S phase due to CHK1 phosphorylation.

Nevertheless, there are limitations in our study. First, HSF1 generally stands as a transcription factor to regulate multiple gene networks, but the upstream signaling pathway responsible for activating HSF1 requires further elucidation. Besides, although HHT reduces the elevation of HSF1 stimulated by HSP90 inhibitors, the efficacy of HHT on HSP90-resistant cells or

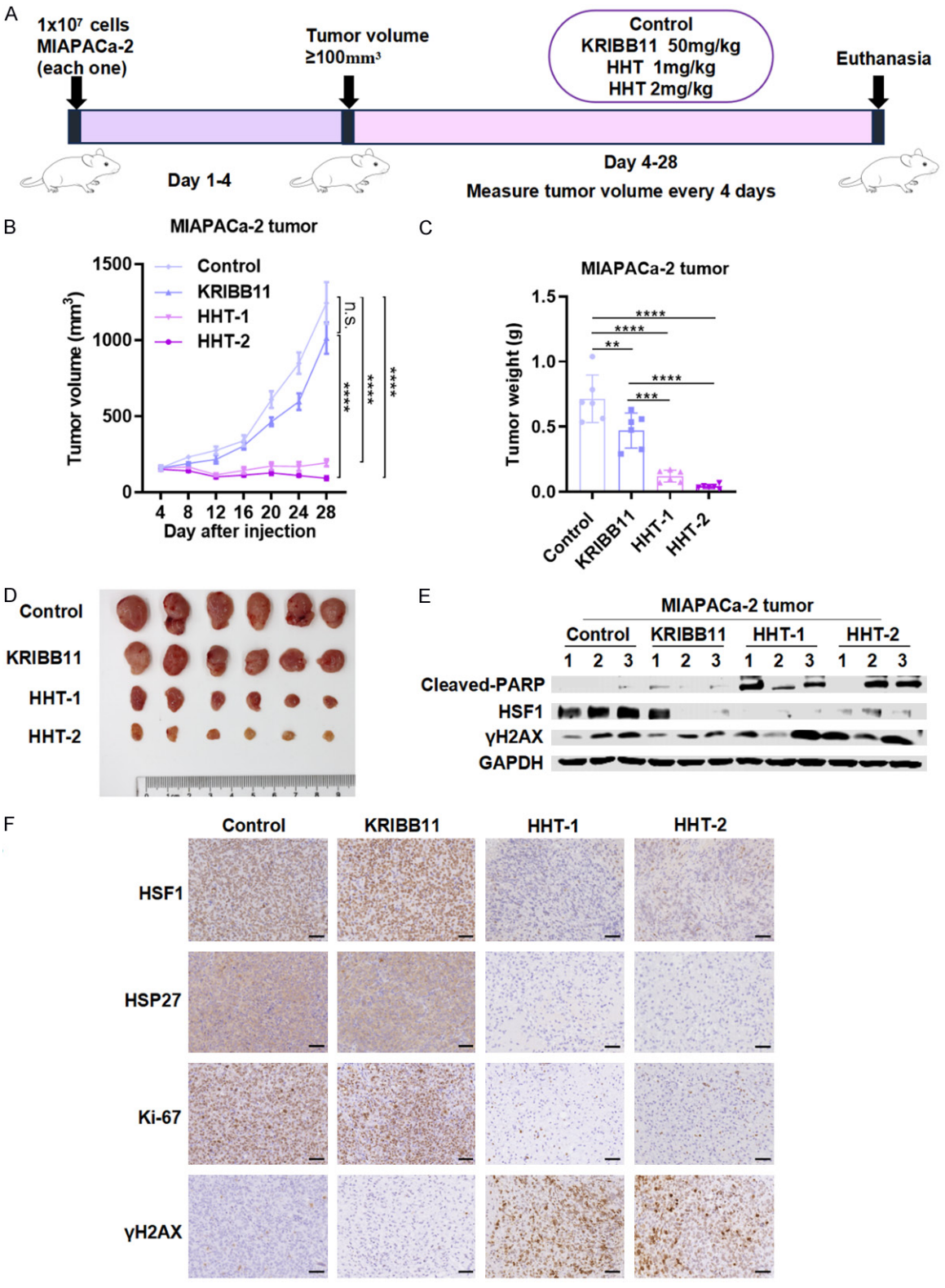

Figure 7. HHT blocks pancreatic cancer growth in *vivo*. A. BALC/NUDE mouse was subcutaneously inoculated with 1 × 10^7 MIAPACa-2 cells. B. The MIAPACa-2 tumor volume was measured every 4 days (n=6 per group). C, D. Tumors were stripped, weighted, and photographed at the end of the experiment. E. Three tumor samples were selected from each of the four groups and western blot was performed to detect the expressions of cleaved-PARP, HSF1 and γH2AX. F. Immunostaining staining for HSF1, HSP27, γH2AX, and Ki-67 in MIAPACa-2 tumors. Scale bar, 50 μm.

tumors remains uncertain. The potential synergistic effects of combining HHT with HSP90 inhibitors are promising but require more exploration. Moreover, while HHT has been preliminarily confirmed to bind to HSF1, additional investigation is required to elucidate the interaction domains and specific amino acid residues involved. Beyond the scope of PC, HSF1 dysregulation is implicated in other malignancies such as hepatocellular carcinoma, prostate cancer, breast cancer, and ovarian cancer. Therefore, it is imperative to extend the study of HHT's inhibitory effects to these cancers as well.

Acknowledgements

This work was supported by grants from the Science and Technology Commission of Shanghai Municipality (grant no: 21S11902000) and the Shanghai Oriental Talent Plan Project (2023).

Disclosure of conflict of interest

None.

Address correspondence to: Zhen-Liang Sun, Affiliated Fengxian Hospital, Southern Medical University, 6600 Nanfeng Road, Fengxian District, Shanghai 201499, P. R. China. Tel: +86-21-57416150; E-mail: zhenliang6@126.com; Zheng-Fang Yi, Institute of Biomedical Sciences, East China Normal University, 500 Dongchuan Road, Shanghai 200241, P. R. China. Tel: +86-21-5434-5016; E-mail: zfyi@bio.ecnu.edu.cn

References

[1] Dong B, Jaeger AM and Thiele DJ. Inhibiting heat shock factor 1 in cancer: a unique therapeutic opportunity. Trends Pharmacol Sci 2019; 40: 986-1005.
[2] O'Malley J, Kumar R, Inigo J, Yadava N and Chandra D. Mitochondrial stress response and cancer. Trends Cancer 2020; 6: 688-701.
[3] Li J, Labbadia J and Morimoto RI. Rethinking HSF1 in stress, development, and organismal health. Trends Cell Biol 2017; 27: 895-905.
[4] Kurop MK, Huyen CM, Kelly JH and Blagg BSJ. The heat shock response and small molecule regulators. Eur J Med Chem 2021; 226: 113846.
[5] Kovács D, Kovács M, Ahmed S and Barna J. Functional diversification of heat shock factors. Biol Futur 2022; 73: 427-439.
[6] Gomez-Pastor R, Burchfiel ET and Thiele DJ. Regulation of heat shock transcription factors and their roles in physiology and disease. Nat Rev Mol Cell Biol 2018; 19: 4-19.
[7] Sharma C and Seo YH. Small molecule inhibitors of HSF1-activated pathways as potential next-generation anticancer therapeutics. Molecules 2018; 23: 2757.
[8] Kijima T, Prince T, Neckers L, Koga F and Fujii Y. Heat shock factor 1 (HSF1)-targeted anticancer therapeutics: overview of current preclinical progress. Expert Opin Ther Targets 2019; 23: 369-377.
[9] Kovács D, Sigmond T, Hotzi B, Bohár B, Fazekas D, Deák V, Vellai T and Barna J. HSF1Base: a comprehensive database of HSF1 (heat shock factor 1) target genes. Int J Mol Sci 2019; 20: 5815.
[10] Alasady MJ and Mendillo ML. The multifaceted role of HSF1 in tumorigenesis. Adv Exp Med Biol 2020; 1243: 69-85.
[11] Fang Z, Meng Q, Xu J, Wang W, Zhang B, Liu J, Liang C, Hua J, Zhao Y, Yu X and Shi S. Signaling pathways in cancer-associated fibroblasts: recent advances and future perspectives. Cancer Commun (Lond) 2023; 43: 3-41.
[12] Jia G, Wu W, Chen L, Yu Y, Tang Q, Liu H, Jiang Q and Han B. HSF1 is a novel prognostic biomarker in high-risk prostate cancer that correlates with ferroptosis. Discov Oncol 2023; 14: 107.
[13] Qin T, Chen K, Li J, Qian W, Xiao Y, Wu E, Ma J, Chen Z, Wang Z, Ma Q and Wu Z. Heat shock factor 1 inhibition sensitizes pancreatic cancer to gemcitabine via the suppression of cancer stem cell-like properties. Biomed Pharmacother 2022; 148: 112713.
[14] Shen Z, Yin L, Zhou H, Ji X, Jiang C, Zhu X and He X. Combined inhibition of AURKA and HSF1 suppresses proliferation and promotes apoptosis in hepatocellular carcinoma by activating endoplasmic reticulum stress. Cell Oncol (Dordr) 2021; 44: 1035-1049.
[15] Vydra N, Toma-Jonik A, Janus P, Mrowiec K, Stokowy T, Głowala-Kosińska M, Sojka DR, Olbryt M and Widłak W. An increase in HSF1 expression directs human mammary epithelial cells toward a mesenchymal phenotype. Cancers (Basel) 2023; 15: 4965.
[16] Solimini NL, Luo J and Elledge SJ. Non-oncogene addiction and the stress phenotype of cancer cells. Cell 2007; 130: 986-8.
[17] Qian W, Chen K, Qin T, Xiao Y, Li J, Yue Y, Zhou C, Ma J, Duan W, Lei J, Han L, Li L, Shen X, Wu Z, Ma Q and Wang Z. The EGFR-HSF1 axis accelerates the tumorigenesis of pancreatic cancer. J Exp Clin Cancer Res 2021; 40: 25.
[18] Dong B, Jaeger AM, Hughes PF, Loiselle DR, Hauck JS, Fu Y, Haystead TA, Huang J and Thiele DJ. Targeting therapy-resistant prostate cancer via a direct inhibitor of the human heat

shock transcription factor 1. Sci Transl Med 2020; 12: eabb5647.
[19] Liang W, Liao Y, Zhang J, Huang Q, Luo W, Yu J, Gong J, Zhou Y, Li X, Tang B, He S and Yang J. Heat shock factor 1 inhibits the mitochondrial apoptosis pathway by regulating second mitochondria-derived activator of caspase to promote pancreatic tumorigenesis. J Exp Clin Cancer Res 2017; 36: 64.
[20] Cheeseman MD, Chessum NE, Rye CS, Pasqua AE, Tucker MJ, Wilding B, Evans LE, Lepri S, Richards M, Sharp SY, Ali S, Rowlands M, O'Fee L, Miah A, Hayes A, Henley AT, Powers M, Te Poele R, De Billy E, Pellegrino L, Raynaud F, Burke R, van Montfort RL, Eccles SA, Workman P and Jones K. Discovery of a chemical probe bisamide (CCT251236): an orally bioavailable efficacious pirin ligand from a heat shock transcription factor 1 (HSF1) phenotypic screen. J Med Chem 2017; 60: 180-201.
[21] Velayutham M, Cardounel AJ, Liu Z and Ilangovan G. Discovering a reliable heat-shock factor-1 inhibitor to treat human cancers: potential opportunity for phytochemists. Front Oncol 2018; 8: 97.
[22] Levi-Galibov O, Lavon H, Wassermann-Dozorets R, Pevsner-Fischer M, Mayer S, Wershof E, Stein Y, Brown LE, Zhang W, Friedman G, Nevo R, Golani O, Katz LH, Yaeger R, Laish I, Porco JA, Sahai E, Shouval DS, Kelsen D and Scherz-Shouval R. Heat shock factor 1-dependent extracellular matrix remodeling mediates the transition from chronic intestinal inflammation to colon cancer. Nat Commun 2020; 11: 6245.
[23] Masuo H, Kubota K, Shimizu A, Notake T, Miyazaki S, Yoshizawa T, Sakai H, Hayashi H and Soejima Y. Increased mitochondria are responsible for the acquisition of gemcitabine resistance in pancreatic cancer cell lines. Cancer Sci 2023; 114: 4388-4400.
[24] Chen K, Qian W, Li J, Jiang Z, Cheng L, Yan B, Cao J, Sun L, Zhou C, Lei M, Duan W, Ma J, Ma Q and Ma Z. Loss of AMPK activation promotes the invasion and metastasis of pancreatic cancer through an HSF1-dependent pathway. Mol Oncol 2017; 11: 1475-1492.
[25] Zaib S, Hayyat A, Ali N, Gul A, Naveed M and Khan I. Role of mitochondrial membrane potential and lactate dehydrogenase a in apoptosis. Anticancer Agents Med Chem 2022; 22: 2048-2062.
[26] Ganguly S, Home T, Yacoub A, Kambhampati S, Shi H, Dandawate P, Padhye S, Saluja AK, McGuirk J and Rao R. Targeting HSF1 disrupts HSP90 chaperone function in chronic lymphocytic leukemia. Oncotarget 2015; 6: 31767-79.
[27] Kijima T, Prince TL, Tigue ML, Yim KH, Schwartz H, Beebe K, Lee S, Budzynski MA, Williams H, Trepel JB, Sistonen L, Calderwood S and Neckers L. HSP90 inhibitors disrupt a transient HSP90-HSF1 interaction and identify a noncanonical model of HSP90-mediated HSF1 regulation. Sci Rep 2018; 8: 6976.
[28] Klein AP. Pancreatic cancer epidemiology: understanding the role of lifestyle and inherited risk factors. Nat Rev Gastroenterol Hepatol 2021; 18: 493-502.
[29] Zhang CY, Liu S and Yang M. Clinical diagnosis and management of pancreatic cancer: markers, molecular mechanisms, and treatment options. World J Gastroenterol 2022; 28: 6827-6845.
[30] Du P, Dai F, Chang Y, Wei C, Yan J, Li J and Liu X. Role of miR-199b-5p in regulating angiogenesis in mouse myocardial microvascular endothelial cells through HSF1/VEGF pathway. Environ Toxicol Pharmacol 2016; 47: 142-148.
[31] Lin Q, Xiao G, Wang G, He Q, Xu L, Qiu P, Tan S, Gong M, Wen J and Xiao X. Heat shock factor 1 in relation to tumor angiogenesis and disease progression in patients with pancreatic cancer. Pancreas 2020; 49: 1327-1334.
[32] Shaashua L, Ben-Shmuel A, Pevsner-Fischer M, Friedman G, Levi-Galibov O, Nandakumar S, Barki D, Nevo R, Brown LE, Zhang W, Stein Y, Lior C, Kim HS, Bojmar L, Jarnagin WR, Lecomte N, Mayer S, Stok R, Bishara H, Hamodi R, Levy-Lahad E, Golan T, Porco JA Jr, Iacobuzio-Donahue CA, Schultz N, Tuveson DA, Lyden D, Kelsen D and Scherz-Shouval R. BRCA mutational status shapes the stromal microenvironment of pancreatic cancer linking clusterin expression in cancer associated fibroblasts with HSF1 signaling. Nat Commun 2022; 13: 6513.
[33] Crake R, Gasmi I, Dehaye J, Lardinois F, Peiffer R, Maloujahmoum N, Agirman F, Koopmansch B, D'Haene N, Azurmendi Senar O, Arsenijevic T, Lambert F, Peulen O, Van Laethem JL and Bellahcène A. Resistance to gemcitabine in pancreatic cancer is connected to methylglyoxal stress and heat shock response. Cells 2023; 12: 1414.

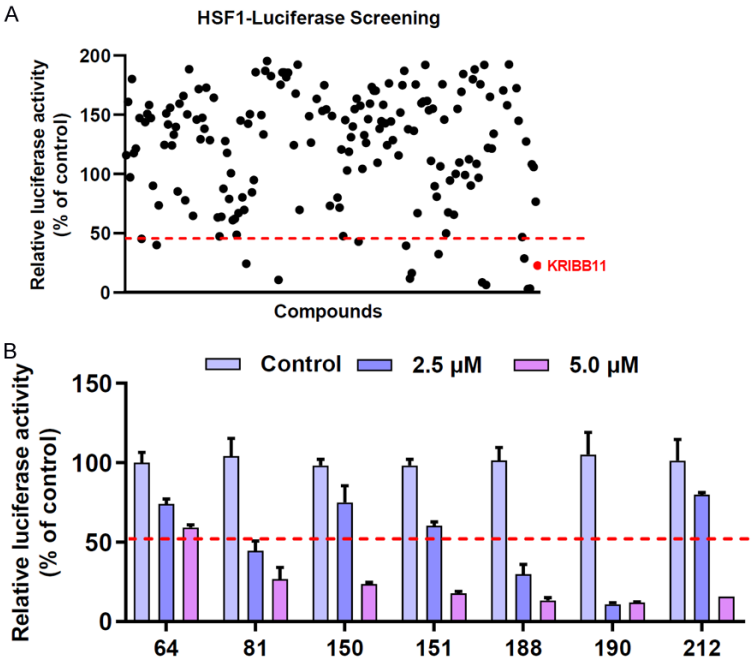

Figure S1. The discovery of HSF1 inhibitors. A. The screening results based on the dual luciferase reporter system. B. Several compounds were founded and HHT was discovered to significantly inhibit luciferase activity.

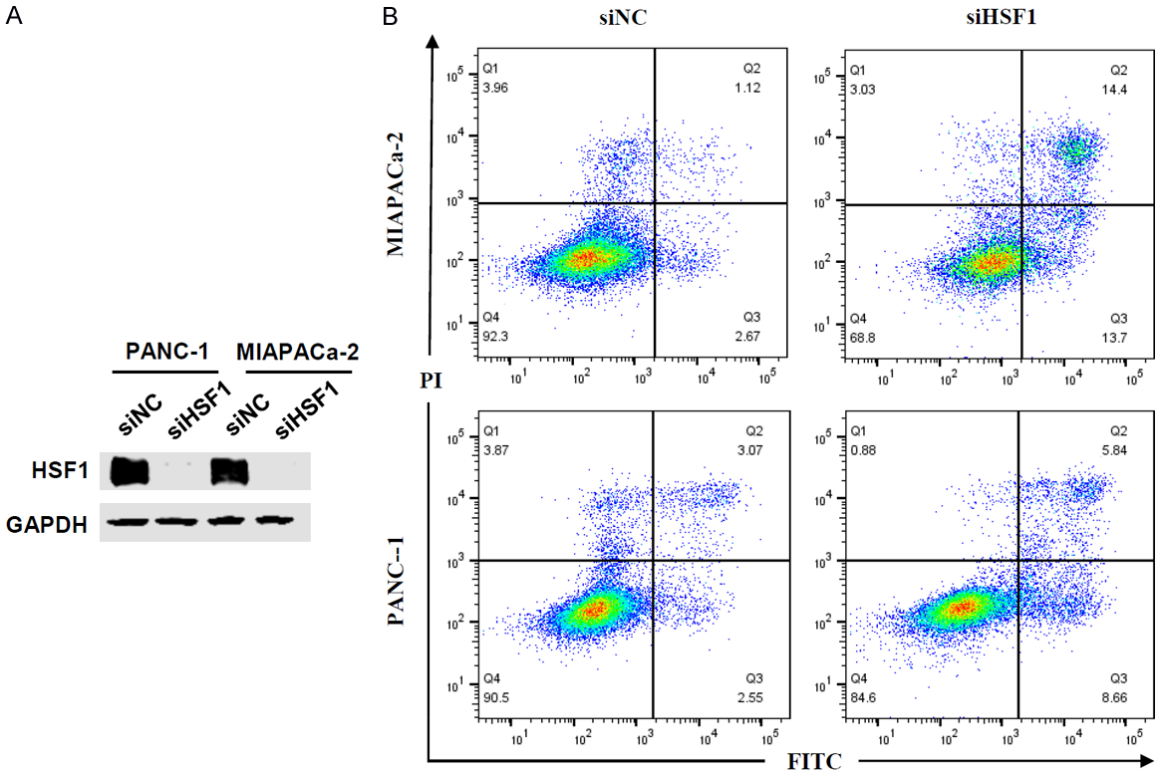

Figure S2. Loss of HSF1 induced pancreatic cancer cells apoptosis. A. Depletion efficacy of HSF1 in PC cells was detected by western blot analysis. B. Cell apoptosis assays of PANC-1 and MIAPACa-2 cells transfected with HSF1 siRNA using flow cytometry.

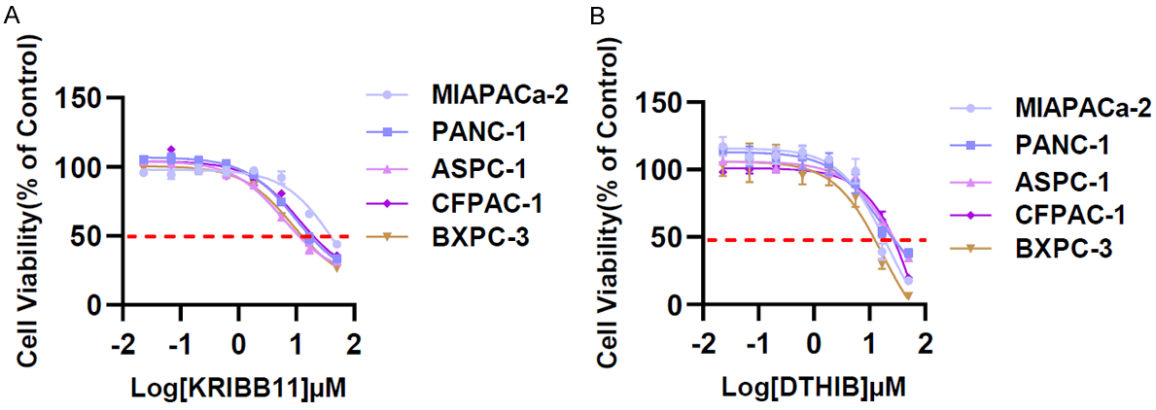

C

Cells	IC_{50} (μM)		
	HHT	KRIBB11	DTHIB
MIAPACa-2	0.0199±0.0015	>10	>10
PANC-1	0.0179±0.0011	>10	>10
ASPC-1	0.0725±0.0040	>10	>10
CFPAC-1	0.0575±0.0019	>10	>10
BXPC-3	0.5969±0.0346	>10	>10
HPNE	0.3227± 0.0261		

Figure S3. Inhibitory of positive drug in pancreatic cancer cells. A. KRIBB11 inhibitory activities against PC cells proliferation. B. DTHIB inhibitory activities against PC cells proliferation. C. IC_{50} summary of HHT, KRIBB11 and DTHIB.

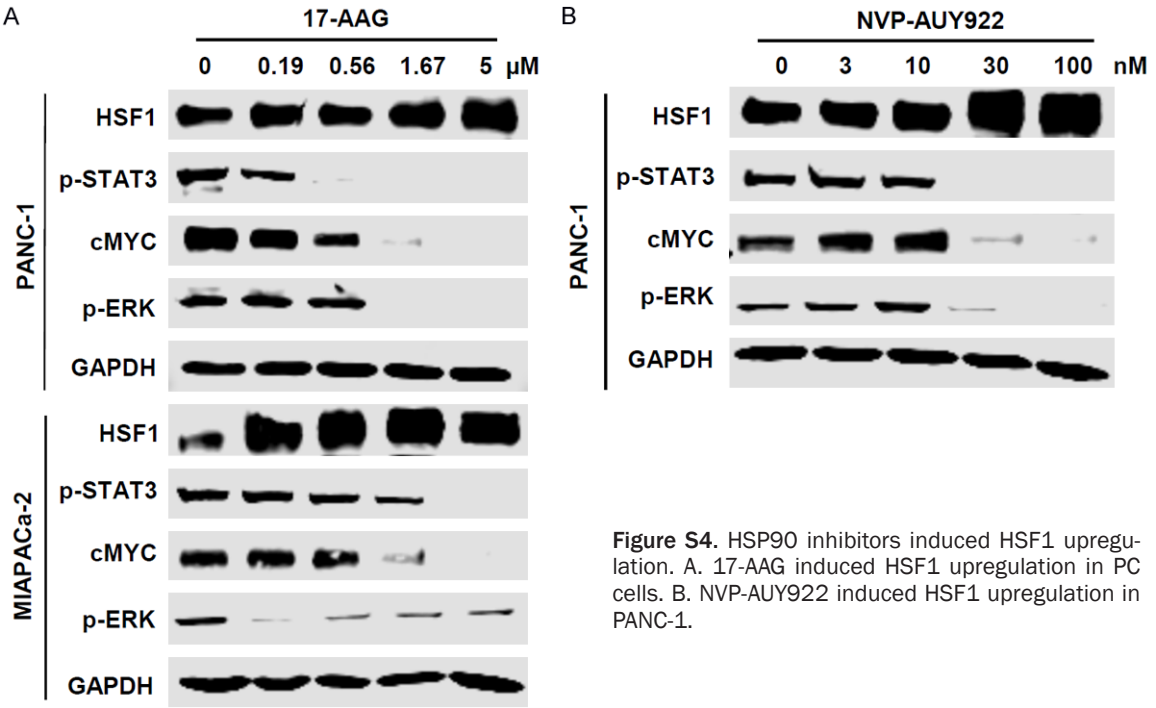

Figure S4. HSP90 inhibitors induced HSF1 upregulation. A. 17-AAG induced HSF1 upregulation in PC cells. B. NVP-AUY922 induced HSF1 upregulation in PANC-1.

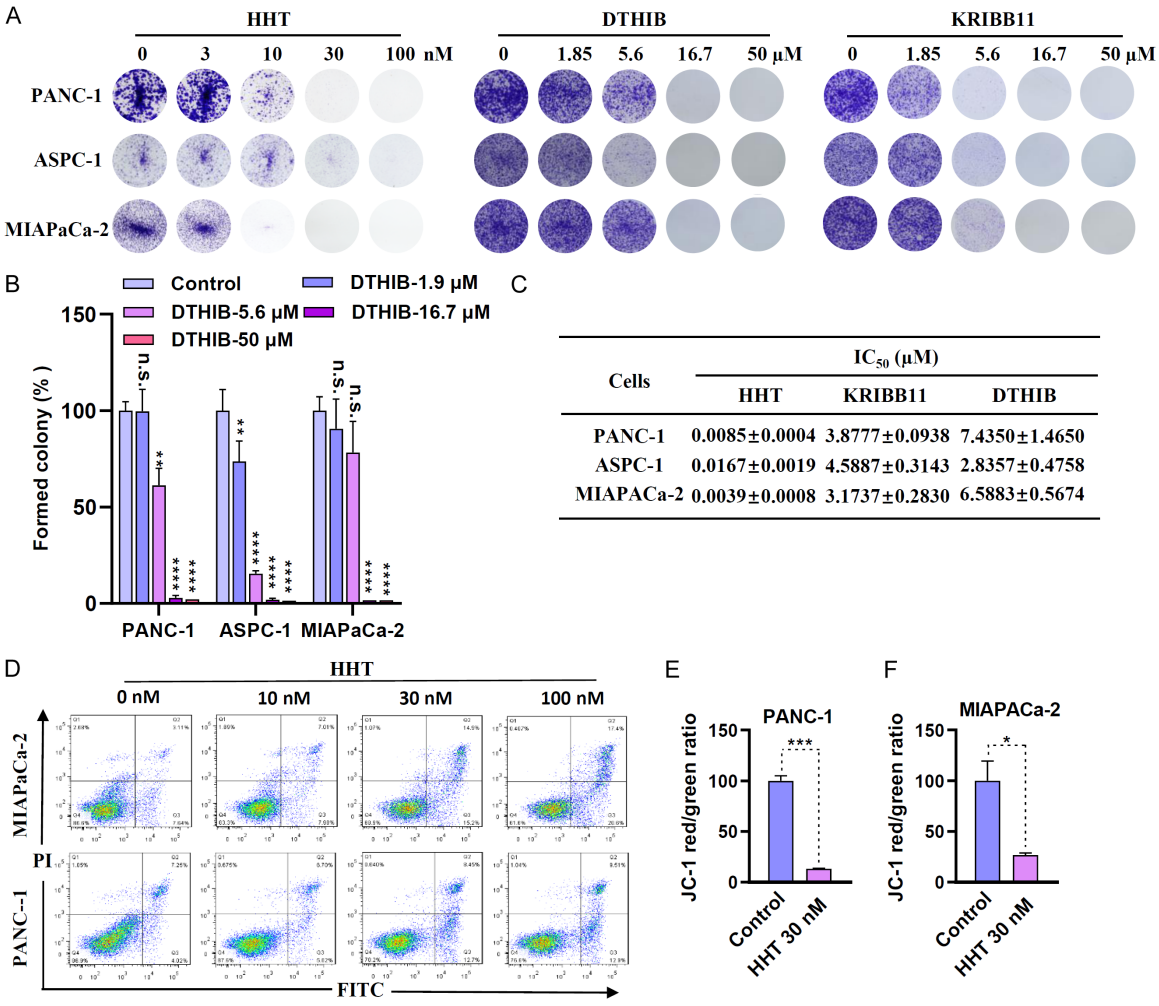

Cells	IC_{50} (μM)		
	HHT	KRIBB11	DTHIB
PANC-1	0.0085±0.0004	3.8777±0.0938	7.4350±1.4650
ASPC-1	0.0167±0.0019	4.5887±0.3143	2.8357±0.4758
MIAPACa-2	0.0039±0.0008	3.1737±0.2830	6.5883±0.5674

Figure S5. HHT significantly inhibited pancreatic cancer cells colony formation and induced apoptosis. A, B. HHT, KRIBB11 and DTHIB inhibited PC cells colony formation. PC cells were seeded in 6-well plates, and treated with different doses of HHT, KRIBB11 and DTHIB. C. IC_{50} summary of HHT, KRIBB11 and DTHIB on inhibiting PC cells colony formation. D. PC cells were treated with HHT for 48 h, apoptotic cells were detected by flow cytometry. E, F. PANC1-1 and MIAPACa-2 were treated with or without 30 nM for 48 h, mitochondrial membrane potential was quantified and statistical analysis was conducted.

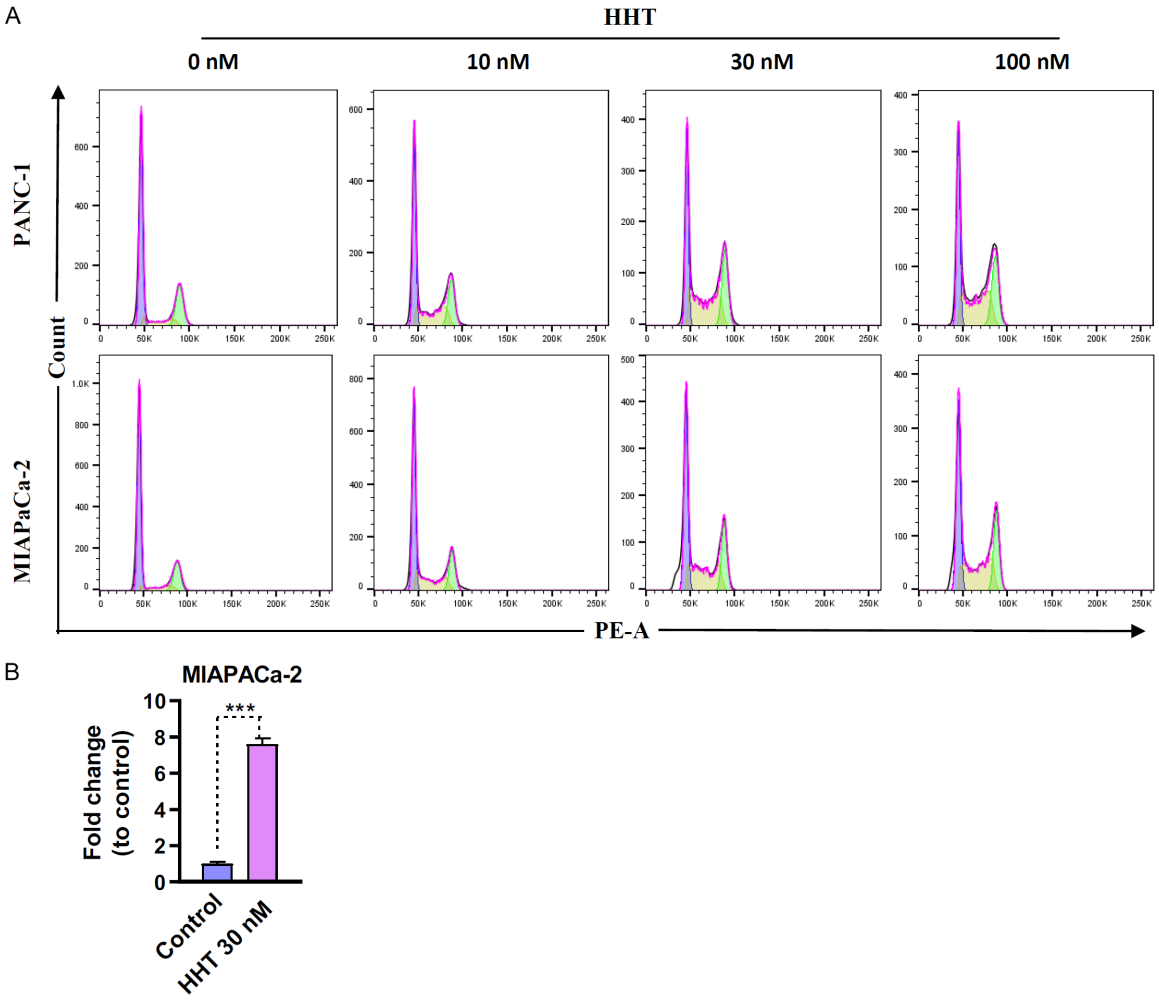

Figure S6. HHT significantly caused pancreatic cancer cells cycle arrest. A. PC cells were treated with HHT for 48 h, cell cycle distribution were detected by flow cytometry. B. γH2AX integrated density were calculated by Image J software. Fold change of integrated density were showed in the dosing group compared with the control group.

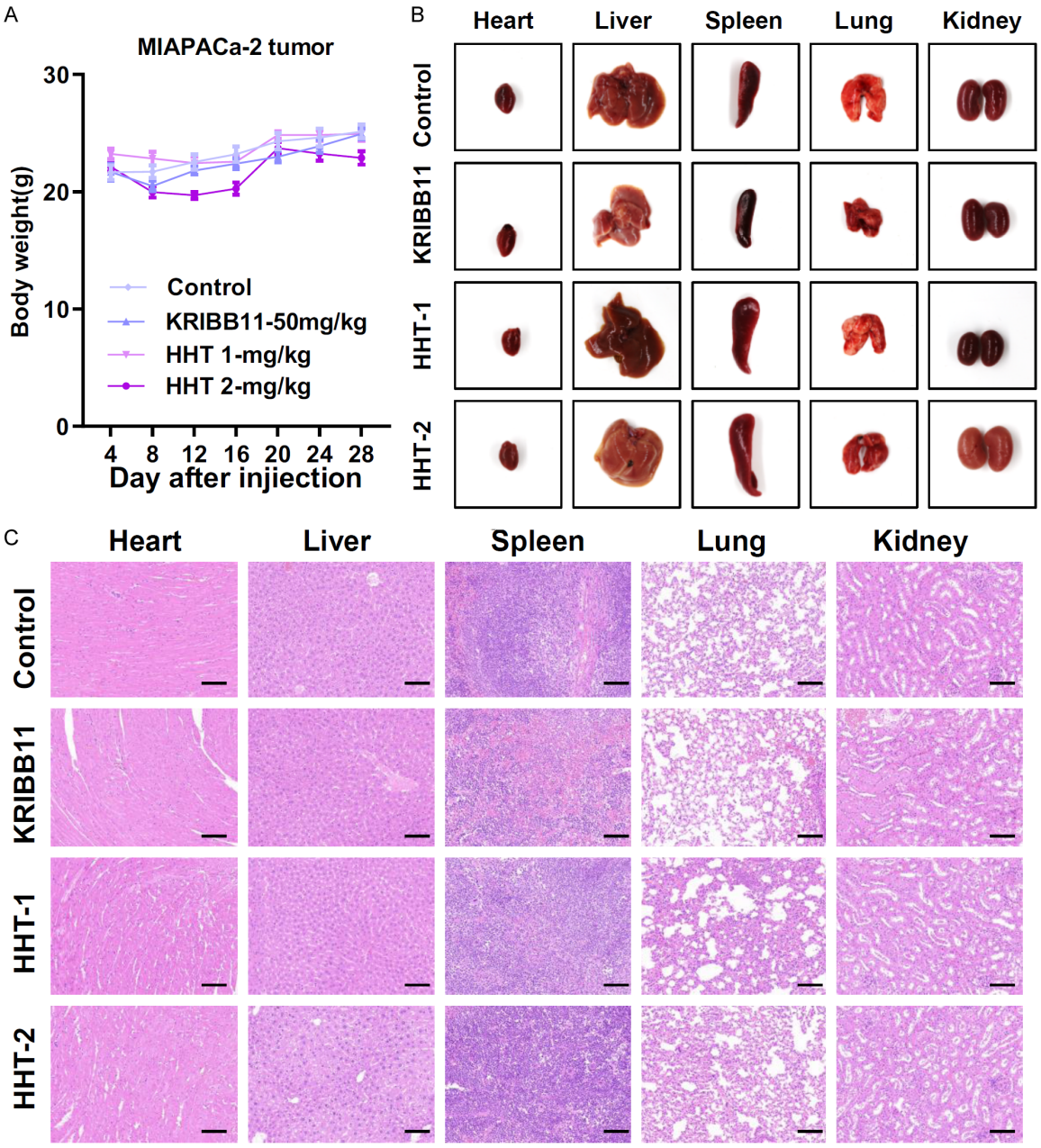

Figure S7. HHT was well-tolerated in *vivo*. A. Body weight in different treatment groups of mice was measured every 4 days (n=6). B. The mice were sacrificed after treatment for 24 days and the organs were excised and photographed. C. H&E staining of heart, liver, spleen, lung, kidney tissues of both groups. Scale bar, 100 μm.